Tailoring cellulose nanocrystals rheological behavior in aqueous suspensions through surface functionalization with polyethyleneimine

Cite as: Phys. Fluids **31**, 021207 (2019); https://doi.org/10.1063/1.5046669
Submitted: 29 June 2018 . Accepted: 06 September 2018 . Published Online: 28 December 2018

Dhriti Khandal, Bernard Riedl, Jason R. Tavares, Pierre J. Carreau, and Marie-Claude Heuzey

Tailoring cellulose nanocrystals rheological behavior in aqueous suspensions through surface functionalization with polyethyleneimine

Cite as: Phys. Fluids 31, 021207 (2019); doi: 10.1063/1.5046669
Submitted: 29 June 2018 • Accepted: 6 September 2018 •
Published Online: 28 December 2018

Dhriti Khandal,[1] Bernard Riedl,[2] Jason R. Tavares,[1] Pierre J. Carreau,[1] and Marie-Claude Heuzey[1,a)]

AFFILIATIONS

[1] Department of Chemical Engineering, CREPEC—Research Center on High Performance Polymer and Composite Systems, Polytechnique Montreal, Montreal, Quebec H3T 1J4, Canada

[2] Département des Sciences du Bois et de la Forêt, Faculté de Foresterie, Géographie et Géomatique, Université Laval, Quebec, Quebec G1V 0A6, Canada

[a)] Author to whom correspondence should be addressed: marie-claude.heuzey@polymtl.ca. Tel.: +1 (514) 340-4711 ext. 5930.

ABSTRACT

This paper reports the surface modification of commercially available cellulose nanocrystals (CNCs) using polyethyleneimine (PEI) by means of non-covalent electrostatic interaction between the negatively charged sulfate groups of CNCs and positively charged amine functionalities of PEI. The modification, carried out in an aqueous medium, results in a stable CNC-PEI suspension with no phase separation that exhibits interesting rheological behavior due to bridging-type inter-particle interactions. The Newtonian 3% (w/w) CNC suspension evolves into a non-Newtonian gel system after modification with PEI with a consequent increase of almost three decades in complex viscosity. Pre-shearing of the 3% (w/w) CNC-PEI suspension resulted in the loss of the linear viscoelastic properties with increasing shear rate, as would be expected from the breaking of the inter-particle network. However, the system gradually re-established the inter-particle network in less than an hour to give the original rheological parameters. The effect of PEI on the rheological properties was attributed to the physical adsorption of PEI chains on the CNC particles, examined by dynamic light scattering, zeta potential, X-ray photoelectron spectroscopy, elemental analyses, and isothermal adsorption studies. The modified CNC-PEI particles did not show any significant change in the particle morphology compared to the unmodified CNCs, as observed from transmission electron microscope images.

INTRODUCTION

The microfibrils obtained from wood after the removal of lignin and hemicelluloses are basically cellulose chains held together by H-bonding, resulting in highly ordered and crystalline regions alternated by disordered amorphous regions (Habibi *et al.*, 2010; Moon *et al.*, 2011; and Kalia *et al.*, 2011). The amorphous regions of these microfibrils are broken down by mechanical treatment or sulfuric acid hydrolysis, to extract the crystalline regions as fine rod-shaped cellulose nanocrystals (CNCs). Therefore, CNCs are bioresource-derived nanoparticles, and they are known for their high aspect ratio, large surface area, high strength, and anisotropic properties with a tendency to adopt directional orientation (Marchessault *et al.*, 1959). These particles provide a green alternative for potential applications in different fields ranging from reinforcing polymer matrices (Girouard *et al.*, 2015; Bagheriasl *et al.*, 2016; Beuguel *et al.*, 2018a; and Li *et al.*, 2016) to the development of dispersions and Pickering emulsions (Kalashnikova *et al.*, 2013; Wena *et al.*, 2014; and Hu *et al.*, 2015), aerogels, and coatings (Hoeger *et al.*, 2011 and France *et al.*, 2017), improving electrical conductivity of conducting polymers (Meulendijks *et al.*, 2017) and fillers for concrete (Cao *et al.*, 2016). Apart from their remarkable physical attributes, the CNCs are also biocompatible, biodegradable and have low toxicity, making them good candidates for biomedical applications, such as tissue engineering (Millon and Wan, 2006; Guise and Fangueiro, 2016; and Sabra *et al.*, 2017).

Despite CNCs having desirable physical properties, they do not possess suitable surface properties required for certain applications, such as appropriate hydrophobicity for dispersion in non-polar media or polymer matrices (Eyley and Thielemans, 2014). Hence, surface modifications of CNCs have been carried out to improve the interfacial interaction with polymer matrices, whereby the reinforcing properties were further enhanced (Peresin *et al.*, 2014 and Zhao *et al.*, 2017). Reactive functionalities can also chemically be grafted onto the hydroxyl groups on the surface of CNCs, which allowed them to eventually react with the polymer (Xu *et al.*, 2008 and Girouard *et al.*, 2016). In one study, the CNCs were chemically modified to bear cationic functionalities and then used for the preparation of carboxy-methyl cellulose films by means of solvent casting. The solubility of both the cationically modified CNCs and negatively charged carboxymethyl cellulose in water allowed for a good dispersion of the nanoparticles in the matrix, while the electrostatic interaction between the oppositely charged species allowed for good interfacial interaction and improved mechanical properties of the resulting films (Li *et al.*, 2016). Other surface modifications, such as grafting fluorescent groups onto CNCs to allow bioimaging, have been reported (Dong and Roman, 2007), while a solvent-free approach of modification has been developed by a technique known as photo-initiated chemical vapor deposition (PICVD) that could be an interesting option for large-scale covalent modification (Javanbakht *et al.*, 2016).

While the moderate hydrophilicity of CNCs allows them to be easily dispersed in polar matrices such as polyvinyl alcohol (Abitbol *et al.*, 2011 and Jorfi *et al.*, 2013) and polyethylene glycol (Beuguel *et al.*, 2018a), without any need for prior surface modification, CNCs have also been modified to have improved polarity in terms of surface charge for applications requiring good suspension stability in water; for example, CNCs were oxidized using (2,2,6,6-tetramethylpiperidine-1-oxyl radical) (TEMPO)-mediated oxidation to introduce carboxylate functionalities on the surface, which allowed better suspension stability (Yang *et al.*, 2015). In the case of CNCs obtained from sulfuric acid treatment, there are sulfate half ester groups formed on the surface, which impart a negative charge to the CNCs once dispersed in water. These particles have good suspension stability in water lasting for days without any agglomeration due to electrostatic repulsion between the particles (Beuguel *et al.*, 2018b). The sulfate bearing CNCs have also been reported to act as anti-coagulant agents in blood by mimicking the naturally occurring heparin in terms of charge density (Ehmann *et al.*, 2014).

Certain suspensions of surface modified CNCs can form hydrogels, which are particularly interesting as the suspension characteristics depend not only on the concentration of the particles but on their surface properties as well. The 4% (w/w) suspension CNCs bearing sulfate groups were reported to result in hydrogels after an autoclave treatment of 20 h at 80 °C or 4 h at 120 °C, which was explained to be caused by the desulfation of the particles and the free sulfate groups acting as inter-particle crosslinks (Lewis *et al.*, 2016). Suspensions of cationically modified CNCs have also been reported to result in hydrogels under certain conditions. Positive charges were rendered on CNCs by covalently grafting epoxypropyltrimethylammonium chloride on their surface, and at a certain concentration, these modified CNCs in water were reported to form a weak hydrogel that lost its gel-behavior after shearing (Hasani *et al.*, 2008). Thus, depending on the kind of surface modification, the CNC suspensions can be tailored for specific rheological properties.

Non-covalent surface modification of CNCs is of interest because it does not involve the use of any coupling agents or solvent purification processes, which can bring about toxicity and environmental concerns. This type of modification relies on the electrostatic interaction between the negatively charged CNCs with an appropriately chosen cationic additive. The non-covalent surface modification of CNCs is usually carried out in a solvent that both solubilizes the additive (adsorbing agent) and disperses the CNCs. While this method appears to be easy to implement and would be industrially friendly, the resulting modification is accompanied by an instant phase separation of the nanoparticles because of decreased surface polarity (Heux *et al.*, 2002 and Kaboorani and Riedl, 2015), leading to the loss of rheological properties of the suspension.

Given the advantages of CNCs obtained from sulfuric acid treatment, namely, their availability at a commercial scale, good dispersion in water, and possibility of non-covalent modification, we decided to investigate the surface modification of these particles in an aqueous medium using a suitable cationic additive and study the rheological properties of the resulting aqueous suspensions. Polyethyleneimine (PEI) was chosen as the cationic polymer for this non-covalent surface modification as it is water soluble, is commercially available in both linear and branched forms, and has been reported for numerous applications such as a low toxicity cross-linker (Reddy *et al.*, 2003; Jia *et al.*, 2010; and Sun *et al.*, 2011), a binding or fixing agent that improves the effluent quality of the pulp and the print quality on paper in the pulp and paper industry (Wang *et al.*, 2016), for drug delivery and other biomedical applications (Lin and Dufresne, 2014), for its anti-microbial properties (Azevedo *et al.*, 2014), and a chelation agent with heavy metals (Kobayashi *et al.*, 1987). PEI has also been chemically bound to TEMPO-oxidized CNCs to aid their dispersion in polymers such as epoxy resins (Zhao *et al.*, 2017) and used to crosslink cellulose nanofibrils to create biomedical scaffolds (Alexandrescu *et al.*, 2013). The interactions between macroions, such as charged DNA, RNA, silica particles, and cell membrane proteins due to the presence of an oppositely charged polyelectrolyte (e.g., PEI) are called bridging interactions (Podgornik, 2004). This type of molecular interaction allows PEI to be used in gene delivery (Xia *et al.*, 2009 and Ortega-MuCoz *et al.*, 2016) and cell attachment (Vancha *et al.*, 2004). PEI acts as a mediator and reduces the interparticle distance between the negatively charged macroions (Popto-shev and Claesson, 2002). Linear PEI chains are known to adopt a random coil conformation in water, while branched PEI is reported to have a spherical-type conformation

(Suh *et al.*, 1994). Since CNCs would have a large effective surface area and negative charges when properly dispersed in water, they are likely to consume a large quantity of PEI during the modification, which would eventually result in loss of morphology of the particles along with phase separation from the suspension. Therefore, it was decided to focus on preparing stable aqueous suspensions using low amounts of branched PEI (greater charge density than linear PEI) and analyze the rheological properties of the resulting aqueous CNC-PEI suspensions.

MATERIALS

Spray-dried CNCs obtained from sulfuric acid hydrolysis of wood pulp were provided by CelluForce (Montreal, Canada) (Beck *et al.*, 2012) and used as such. Similar to previous reported work on these CNCs, they were found to have approximately 3.5 half-ester sulfate groups per 100 anhydrose glucose units from X-ray photoelectron spectroscopy (XPS) analysis, corresponding to ~1% degree of substitution (given three hydroxyl groups per anhydrose glucose unit) (Sojoudiasli *et al.*, 2017 and Beuguel *et al.*, 2018b).

The branched PEI purchased from Sigma Aldrich Canada of 99% purity with $\overline{M}_w$ of 25 000 g/mol and polydispersity of ~2.5 was used as received. All preparations were carried out in MilliQ water of resistivity 18.2 MΩ cm.

METHODS

Preparation of CNC and CNC-PEI suspensions

A stable and clear 5% (w/w) CNC suspension was prepared by dispersing 2 g of CNCs in 40 ml of MilliQ water using an ultrasonic homogenizer (Cole-Parmer model CP505 500 W) equipped with a Sonics & Materials VCX500 tapered tip probe. To prevent heating of the suspension during the ultrasonication treatment, the suspension was placed in an ice bath and no more than 2000 J of energy was applied at one time. A total energy of 10 000 J/g of CNC at a power of 28 W using a pulse cycle of 5 s ON and 2 s OFF afforded a complete dispersion of the CNCs (Beuguel *et al.*, 2018b) with no visible agglomerates. This 5% (w/w) suspension was then diluted to 1% (w/w) and 3% (w/w) for the preparation of CNC-PEI suspensions.

A 1% (w/w) solution of PEI was prepared by dissolving 0.1 g in 10 ml of MilliQ water at 50 °C with 30 min of magnetic stirring. A known volume of this PEI solution was added to 1% (w/w) or 3% (w/w) of the clear CNC suspension (prepared above) to carry out the modification and obtain the CNC-PEI suspension. The addition of PEI solution to the well dispersed CNC suspensions was always found to result in an instantaneous phase separation of the nanoparticles from the suspension with visible agglomerates that did not break even upon vigorous shaking. However, the application of sonication during the introduction of PEI into the CNC suspension was found to result in a clear dispersion with no evidence of agglomerate formation and no phase separation for several days. The amount of energy applied during the addition of PEI to the CNC suspension was also important. An energy lower than 5000 J/g of CNCs in the suspension would result in a gradual phase separation, though to a lesser degree than when no sonication was applied. An energy of 5000 J/g of CNC afforded a stable suspension regardless of whether the suspension was made using a dilute 1% (w/w) of CNCs or a more concentrated 3% (w/w) of CNCs in water.

The amount of PEI used for the modification was calculated in terms of g per g of CNC in the final suspension. To simplify the presentation, all suspensions are defined as CNC/PEI (x/y) where x is the weight % (w/w) of CNCs in the suspension and y is the concentration of PEI used in g PEI per g of CNCs. Thus, to prepare 50 ml of CNC-PEI (3/0.01) suspension, 30 ml of 5% (w/w) CNC suspension (i.e., 1.5 g of CNCs) was diluted with 18.5 ml of MilliQ water followed by addition of 1.5 ml of 1% (w/w) PEI solution (i.e., 0.015 g of PEI) and application of 7500 J (for 1.5 g of CNC) of ultrasonication energy. The resulting suspension was clear with a white tinge and showed no apparent phase separation. The same procedure was followed to prepare CNC/PEI (1/0.005), (1/0.01), (1/0.02), (3/0.005), (3/0.01), (3/0.02), and (3/0.05) suspensions.

Since CNC-PEI modification requires an additional ultrasonication treatment of 5000 J/g of CNCs, the unmodified CNC suspension was also treated with this additional energy after dilution to 1% or 3% (w/w) concentration to ensure comparative analysis.

The pH of the CNC suspensions obtained using ultrasonication energy of 10 000 J/g of CNC was always found to vary between 6.7 and 7.1 for different batches. An additional 5000 J/g of CNC did not alter the pH of the suspension. Thus, the ultrasonication energy required for the preparation of CNC-PEI suspensions was considered to not cause damage to the particles or dislodge the sulfate groups from the surface, which would have resulted in a decrease in the pH of the suspension and also affected the surface charges (see the section titled DLS and zeta potential). This confirms our previously reported observation where the ultrasonication performed in ice-cold conditions at a power of 28 W did not result in desulfation (Beuguel *et al.*, 2018b).

Due to the mildly basic character of PEI, the pH of the CNC-PEI suspensions was found to show a slight increase depending on the amount of PEI used for the modification. The trace amounts of 0.005 g of PEI per g of CNCs did not lead to any significant changes in the pH of the CNC suspension (pH being around 6.9-7.3) while the pH of suspensions made using 0.01, 0.02, and 0.05 g of PEI per g of CNCs was found to vary between 7.5 and 8.2.

To obtain dried particles of unmodified CNCs and CNC-PEI, the suspensions were freeze-dried using a Labconco FreeZone Plus 2.5 L Cascade Benchtop freeze dry system after being refrigerated at −20 °C for 3 days. The CNC/PEI freeze-dried particles will be represented as CNC/PEI-y(fd), where y is the concentration of PEI used in g PEI per g of CNCs and "fd" is for freeze-dried.

DLS and zeta potential measurements

The freshly prepared suspensions of CNCs and CNC-PEI were diluted to 0.05% and 0.1% (w/v) concentrations in MilliQ water for the dynamic light scattering (DLS) and zeta potential measurements on the Malvern Zetasizer Nano-S (ZS) and Malvern Zetasizer Nano-ZSP, respectively, at 25 °C. The DLS measurement was carried out on the suspensions as prepared after the required dilution and no pH adjustment was performed before or after dilution. The detection angle for the DLS measurement was 173°, and the correlation factor for these dilutions was around 0.7–0.8, which is indicative of a sufficient particle concentration for reliable data. The suspensions were analyzed in duplicate and, for each sample, three measurements of 15 runs each were carried out with a delay of 30 s for equilibration. The peak position for different particle sizes and their respective area percentages were studied along with the Z_{av} (harmonic mean of scattered intensity of the particle) and polydispersity index (PDI) as calculated by the Malvern Zetasizer software.

For the zeta potential measurements, the net surface charge of the CNC and CNC-PEI particles was analyzed from the electrophoretic mobility using the Smoluchowski equation. Since charges of PEI would be pH dependent, the ζ-potential measurements for 0.05% and 0.1% (w/v) dilutions of the suspensions were also carried out after adjusting their pH to 3 and 10 using freshly prepared 0.1M HCl and 0.1M NaOH solutions, respectively. Since the particles can be affected by the electric current flow during the ζ-potential measurements, each sample was analyzed in triplicate to calculate the standard deviation.

Isothermal adsorption study

To quantify the adsorption of PEI onto the CNC particles, an isothermal adsorption study involving viscometric analysis similar to a previously reported work (Lenfant *et al.*, 2017) was performed on a CANON-Fenske Ubbelhode viscometer with a capillary diameter of 50 μm. A calibration curve of the relative PEI viscosity and concentration was plotted and fitted with the Kraemer-Huggins equation for intrinsic viscosity. The concentrations used for the calibration curve ranged between 0 and 0.02 g/ml of PEI in MilliQ water. The time of the water flow through the capillary of the viscometer used was 268 s.

For the adsorption study of PEI onto the CNCs, a total of 16 suspensions of CNC-PEI suspensions were made by preparing CNC suspensions in water of concentrations of 0.5% and 1% (w/w) and varying the amounts of PEI in them from 0 to 0.01 g/ml in the final suspensions. These concentrations of PEI corresponded to 0–2 g of PEI per g of CNCs in the suspensions. To recover the unadsorbed PEI from the suspensions, two methods were followed. In the first method, calcium chloride salt was added to the suspensions up to a final concentration of no more than 100 mM. This allowed the precipitation of unadsorbed CNCs and CNC-PEI particles, which were then centrifuged at 13 000 rpm for 30 min. The supernatant containing unadsorbed PEI was then decanted and quantified using the calibration curve. In the second method, the suspensions were first freeze dried and then re-suspended with the same volume of water as used during their preparation. The freeze-dried particles were left to swell in water for 4-5 h before magnetic stirring for 24 h. The freeze-dried CNC-PEI particles remained insoluble in water while allowed the dissolution of any excess PEI. The particles were then centrifuged at 13 000 rpm for 90 min, and the supernatant was collected and quantified for free PEI.

XPS analysis

The atomic percentages of C, O, and N on the surface of the freeze-dried CNCs and CNC-PEI with 0.02 g of PEI per g of the CNC sample were determined at 3.0×10^{-9} Torr pressure via a VG ESCALAB 3 MKII XPS instrument equipped with a Mg Kα source of power 300 W. The samples were analyzed for a surface of 2 mm × 3 mm up to a depth of <10 nm. For the quantitative determination, only the high-resolution spectra of C1s, O1s, and N1s peaks obtained were used. The Shirley method was applied to correct the background contribution.

Elemental analysis

The atomic % of C, N, and H in the freeze-dried CNC and CNC-PEI with 0.01 and 0.02 g of PEI per g of CNC samples was determined using an EuroEA Elemental Analyzer instrument. Approximately 1 mg of the sample was weighed up to an accuracy of 0.01 mg and sealed in a tin cap. Empty tin caps were passed as blank samples to ensure column conditioning. The sample was subjected to a furnace temperature of 980 °C and then transferred to a reactor column (EuroVector E13041) for oxidation to generate NO_x, CO_2, and H_2O, which were then separated on the 2 m-long GC column (EuroVector E11501) placed in an oven at 100 °C. The carrier gas used was He with a flow rate of 115 ± 5 ml/min. The identification of the separated gases from their retention times and their respective quantification from their peak area was done using a calibration curve of acetanilide standard.

TEM analysis

The CNC suspension and 3% (w/w) CNC-PEI with 0.02 g PEI per g of CNC was diluted to approximately 0.001% (w/v) in MilliQ water and sonicated for 4 min in a sonicator bath to sufficiently homogenize the particles after dilution. The circular transmission electron microscope (TEM) support involving a Cu grid with a carbon film was dipped in each suspension and allowed to dry. The grid was then placed in a bright field imaging Jeol JEM 2100F TEM instrument operated at an accelerating voltage of 200 kV to image the particles.

Rheology characterization

The rheological tests were performed on a controlled stress rheometer Anton Paar MCR502 using a double-wall

Couette-flow geometry. The time sweep measurements of 1% w/w CNC and CNC-PEI suspensions did not show any evolution in their rheological properties for over 10 h. The freshly prepared suspensions were transferred to the geometry maintained at 25 °C. A pre-shear of 10 s^{-1} was applied for 100 s followed by a 100 s relaxation time before carrying out frequency sweep tests in small amplitude oscillatory shear (SAOS) between 0.1 and 100 rad s^{-1} at a strain within the viscoelastic linear domain. The steady-shear viscosity was measured by applying shear rates between 0.1 and 500 s^{-1}. Note that no reliable data of the 1% CNC suspensions could be obtained for the steady-state viscosity for a shear rate lower than 20 or 30 s^{-1} and the complex viscosity was found to be affected by inertial effects at frequencies larger than 10 rad/s; hence, no superposition of the η^* and η data could be achieved for these data.

The 3% CNC-PEI suspensions were found to evolve with time into a gel system and, hence, time sweep experiments were performed at 10 °C with a solvent trap placed on the bob of the geometry to prevent solvent evaporation and consequent changes in concentration during the experiments. It is worth noting that the 1% CNC-PEI suspensions did not evolve at 10 °C and hence were studied at 25 °C. Therefore, the 3% CNC-PEI suspensions were characterized at 10 °C, while the 1% (w/w) CNC-PEI suspensions were characterized at 25 °C. The freshly prepared 3% CNC-PEI suspension was transferred to the geometry and a pre-shear at 10 s^{-1} for 100 s was applied before launching the time sweep experiment at 1 rad/s with 1% strain. When the evolution of the rheological properties during time sweep experiments was found to stabilize with no more than 10% changes for around 30-40 min, a frequency sweep test (also at 10 °C) was performed between 0.1 and 100 rad s^{-1} at strains of 1% and 15%. The linear viscoelastic domain of these gel systems extended up to ~18% strain, and thus, the rheology values from frequency sweep tests at 1% and 15% strain were found to be similar. The behavior of the gel system in the non-linear domain was studied for both an increasing shear rate from 1 to 500 s^{-1} and a decreasing shear rate from 500 to 1 s^{-1}.

To study the gel structure after shear deformation, a small angle oscillatory shear (SAOS) test for different applied pre-shear rates was performed. This experiment is similar to the previously reported work on polymer-clay nanocomposites (Mobuchon *et al.*, 2007). In brief, a decreasing shear rate from 500 to 0.1 s^{-1} was applied to the gel of the 3% CNC-PEI containing 0.01 g of PEI per g of CNCs. The system was then subjected to a constant pre-shear of 500 s^{-1} for 60 s to reach steady state and then subjected to SAOS at 1 rad s^{-1} and 1% strain for around 2 h. This was followed by other pre-shear rates at 300, 100, 10, and 1 s^{-1}, each followed by an SAOS study of approximately 2 h.

Re-dispersion of freeze-dried particles in water

The freeze-dried particles (~0.02 g) were suspended with 10 ml water and magnetically stirred for 48 h to allow proper wetting and then ultrasonicated up to 10 000 J/g of CNCs to examine their dispersion on re-introduction of water.

RESULTS AND DISCUSSION

DLS and zeta potential

Both the negatively charged CNCs and the PEI have an affinity for water and, therefore, the DLS and zeta potential analyses of the suspensions can indicate whether PEI chains are adsorbed onto CNCs or if PEI remains as a separate entity in the aqueous phase.

It should be mentioned here that the DLS and zeta potential techniques are meant for spherical particles and do not specifically apply to the rod or needle-shaped CNCs as their electromotive mobility varies along the axis and perpendicular to the axis of the particle. For such non-spherical particles, the particle size as measured by the DLS instrument refers to the size of an equivalent spherical particle (a spherical polystyrene calibration curve pre-existing in the software) having an electromotive mobility similar to the average of the axial and equatorial electromotive mobility of the particle being studied. Also, since the electromotive mobility is a function of surface charge and degree of solvation of the particle, the unmodified CNC and CNC-PEI particles would be different in those respects and, hence, can at least be analyzed only on relative terms. Thus, this analysis was only used as a preliminary indication of the adsorption of PEI onto the CNCs and we will concern ourselves with only the relative changes in the particle size and surface charge of the CNCs in the aqueous suspension before and after modification with PEI rather than laying emphasis on the absolute values of size and surface charge of the particles.

The Z_{av} and PDI values of the CNC particles for various suspensions are summarized in Table I along with the size and area percentages of two peaks (peak 1 and peak 2) that were observed for each suspension. Peak 1 refers to the population of larger particles and peak 2 refers to the comparatively smaller particles in the suspension. Since the CNC-PEI suspensions were found to show the occurrence of these two peaks to more or less in the same proportions as for the unmodified CNC particles, the presence of these two peaks is likely due to particle size heterogeneity in the raw material. The suspensions were prepared in duplicates and their values were not found to differ by more than 15%, which is considered as a reasonable degree of reproducibility for this analysis.

The Z_{av} values reported in Table I (rows 1 and 2) for the unmodified CNCs (~73 nm) confirm the results obtained by Beuguel *et al.* (2018b) for well-dispersed CNCs in water. As can be seen for 1% (w/w) CNC suspension modified with different amounts of PEI (rows 3-5 in Table I), the Z_{av} of the CNC particles increases after modification with PEI and the effect is more important as the amount of PEI increases. Thus, despite the water-soluble nature of PEI and the strong affinity of the CNC hydroxyl and sulphate groups for water, the increases in particle size are an indication of physical

TABLE I. The Z_{av} and PDI for the CNC particles in different aqueous suspensions. Peak 1 refers to the population of particles with larger size and peak 2 for the comparatively smaller size particles. Rows 1-9 correspond to experiments conducted without pH adjustment, whereas for rows 10-12, the pH was adjusted.

				Peak 1		Peak 2	
No.	CNC/PEI (x/y)	Z_{av} (nm)	PDI	Size (nm)	Area %	Size (nm)	Area %
1	(1/0)	73 ± 1	0.41 ± 0.10	136	78	33	22
2	(3/0)	73 ± 2	0.39 ± 0.07	113	73	36	27
3	(1/0.005)	122 ± 3	0.43 ± 0.08	205	75	56	25
4	(1/0.01)	136 ± 4	0.46 ± 0.05	221	75	56	22
5	(1/0.02)	143 ± 2	0.45 ± 0.06	321	80	82	20
6	(1/0.01) after 4 days	156 ± 8	0.52 ± 0.01	400	64	97	36
7	(1/0.02) after 4 days	143 ± 6	0.51 ± 0.02	630	47	126	53
8	(3/0.01)	125 ± 6	0.51 ± 0.03	196	56	82	38
9	(3/0.02)	152 ± 4	0.51 ± 0.04	367	58	87	42
10	0.2% (w/w) PEI pH = 3	197 ± 26	0.45 ± 0.20	439	22	22	57
11	0.2% (w/w) PEI pH = 7	225 ± 32	0.53 ± 0.30	269	71	7	29
12	0.2% (w/w) PEI pH = 10	53.8 ± 23	0.43 ± 0.20	27	65	5	35

adsorption due to electrostatic interaction between CNCs and PEI. When these 1% (w/w) CNC-PEI suspensions were stored for 4 days and re-analyzed (rows 6 and 7 in Table I), the Z_{av} value for the CNC/PEI (1/0.002) suspension did not change, while that of CNC/PEI (1/0.001) showed a small increase. However, the particle size increased almost 2 times for both peaks while the difference between their respective area percentages decreased explaining the slight or null effect on the Z_{av} values. The changes in particle size, which are masked in the Z_{av} values but also observed in the PDI values, are indicative of particle-particle interactions with PEI chains acting as bridges.

The 3% (w/w) CNC-PEI suspensions (rows 8 and 9) also show the same trends observed for the 1% (w/w) CNC-PEI suspensions. The only noticeable difference is in the area proportions of peak 1 and peak 2, where the 3% (w/w) CNC-PEI suspensions have peak areas similar to the CNC-PEI (1/0.01 or 0.02) suspensions analyzed after 4 days. This can be understood from the fact that the 3% (w/w) CNC-PEI suspensions have a smaller inter-particle distance and thus a greater tendency to have bridging-type particle-particle associations than the freshly prepared 1% (w/w) CNC-PEI suspensions.

Usually, in DLS, a PDI of <0.1 refers to a monodisperse particle size population while a PDI >0.8 refers to a highly polydispersed size distribution. In all cases, the PDI was found to vary between 0.4 and 0.5, indicating a moderate degree of polydispersity in the particle size. The fact that the PDI of CNC-PEI suspensions was not significantly different from that of unmodified CNC suspension indirectly indicates a uniform modification of the particles.

Rows 10-12 in Table I report the effects of adjusting the pH of the solution. The Z_{av} at pH 10 is very small, but increases as the pH decreases. The pH of the solution would affect the number of protonated amine functionalities (pK_b ~ 5-6) (Smits *et al.*, 1993 and Suh *et al.*, 1994), thereby affecting the intra-particle repulsion and also the double layer due to solvation with water molecules. As the pH of the solution decreases, the number of protonated moieties would increase resulting in greater solvation, larger double layer, and, hence, larger particle size. The small surface charge on PEI at pH 10 (see zeta potential analysis below) would result in less solvation and smaller size while the greater surface charge at pH 3 and 7 would increase the solvation and thus the size.

The zeta potential values measured for the CNC-PEI suspensions without any pH adjustment and also after pH adjustments to 3, 7, and 10 are summarized in Table II. After the required dilution for analysis, the pH of the suspensions was anywhere between 6.8 and 7.5 for the CNC and CNC-PEI suspensions; thus, the zeta potential values without a pH adjustment have been considered as an approximation to be for pH 7 in Table II.

The zeta potential values for the unmodified CNCs do not vary with a change in the pH, which is coherent with the low pK_a values of sulfate groups (pK_a of HSO_4^- is ~2.4). Being a very weak conjugate base of HSO_4^-, the sulfate group is unlikely to accept a proton even at a pH of 3, and thus, the zeta potential values do not change for the unmodified CNCs regardless of the pH. Also, the near constancy in surface charges at different pH indirectly implies the absence of any desulfation due to the ultrasonication treatment. Had there been desulfation, the sulfuric acid formed as a byproduct would have been neutralized when adjusting the pH of the suspension and CNCs

TABLE II. Zeta potential values for CNC, PEI, and CNC-PEI suspensions at different pH.

	Zeta potential (mV)		
CNC/PEI (x/y)	pH = 7	pH = 10	pH = 3
1/0	−47.6 ± 4	−53.2 ± 3	−46.2 ± 2
3/0	−46.9 ± 2	−51.3 ± 2	−47.3 ± 4
1/0.005	−48.0 ± 1	−51.8 ± 5	−43.6 ± 1
1/0.01	−42.6 ± 1	−49.0 ± 3	−30.0 ± 2
1/0.02	−42.1 ± 1	−51.5 ± 2	−20.6 ± 2
3/0.01	−41.2 ± 1	−41.8 ± 2	−34.4 ± 3
3/0.02	−41.2 ± 1	−45.4 ± 2	−28.8 ± 2
0.2% (w/w) PEI solution	+43 ± 1	+6.7 ± 1	+46 ± 1

would have been observed with lower negative charges at pH 10, which was never observed.

In contrast, the PEI molecule with different amine functionalities has a pK_b ~ 5-6, which would allow protonation and deprotonation of the amine groups above and below pH 5-6. If we are to estimate the percentage of protonated groups using the classical Henderson-Hasselbalch equation for pK_b of amines, a pH of ~7 would imply almost 80%-90% of groups being protonated; a pH of 3 would result in all groups being protonated while a pH of 10 would have only 10%-20% of the groups being protonated. This is reflected in the zeta potential values of the PEI solution (last row in Table II), where the positive charge is similar at pH 7 and 3, but is significantly lower at pH 10. Since the CNC-PEI suspensions have a pH ~ 7-8, there would be enough charge density on PEI for an effective electrostatic attraction with CNCs, which is also corroborated by the DLS analysis above showing particle size increases.

As seen from Table II, all of the CNC-PEI suspensions have an overall negative charge on the particle, though it is less than that of unmodified CNCs. The absolute value of the negative charge on CNCs is almost comparable to the positive charge on PEI (pH 7), but since the amount of PEI used in the present study is much lower than the amount of CNCs in the suspension, we observe a decrease in the negative charge after modification rather than a complete neutralization of charge or a reversal of charge. The decrease in the negative surface charge of CNCs is quite significant at pH 3, which is coherent with the increase in the number of protonated amine functionalities at a low pH. When the pH of CNC-PEI suspension is reduced to pH 3, the unprotonated amine functionalities on the already adsorbed PEI would also develop a positive charge, thereby decreasing further the negative charge on the CNC particles. It should be remembered that the surface charge of the CNC-PEI particles measured by zeta-potential is the net charge of the particles and does not imply the absence of positive charge on the adsorbed PEI. Some chains of the branched PEI may bear protonated amine functionalities simply because they are not directly in contact with the CNC surface.

Thus, collectively looking at the DLS and zeta potential analysis of the CNC-PEI suspensions, we can infer that there is an adsorption of PEI chains onto the CNC particles in the aqueous phase and the modification is quite uniform. Also, even though the surface negative charge of CNCs slightly decreases, there may not be a complete charge neutralization. What is also very interesting about these suspensions is that while the decrease in negative charge of particles is generally known to reduce the inter-particle repulsion and consequently affect the suspension stability, this was not observed for the CNC-PEI suspensions, which remained stable for days.

Isothermal adsorption

To quantify the extent of PEI adsorption, we followed one approach based on the electrostatic charge screening of particles by a suitable salt, in this case calcium chloride that allows the precipitation of the unmodified negatively charged CNCs along with the CNC-PEI particles in the suspension. This method relies on the assumption that the electrostatic interaction between CNC and PEI would remain unaffected in the presence of salt. While the use of calcium chloride salt has been studied before for the adsorption of hydroxyethyl cellulose onto CNCs (Lenfant *et al.*, 2017), it is difficult to confidently extrapolate it to the adsorption of PEI onto CNCs without strong experimental proof. Thus, a second methodology was also studied, which is based on the fact that the CNC-PEI particles do not re-disperse in water after they have been dried (see the section titled Re-dispersion of freeze-dried particles in water).

The concentration of the unadsorbed PEI in the supernatant, collected by both methods, was determined using the calibration curve of PEI shown in Fig. 1. The relative viscosity (η_{rel}) was plotted against the concentration (c_i) of PEI and the data were fitted as per the Huggins-Kraemer equation

$$\ln \eta_{rel} = [\eta]c_i + (K_{HK} - 0.5)[\eta]^2 c_i^2, \quad (1)$$

where the intrinsic viscosity ($[\eta]$) and the Huggins-Kraemer constant (K_{HK}) were found to be 10.7 and 0.77, respectively. Using the Mark-Houwink-Sakurada equation $[\eta] = 0.51\bar{M}_v^{0.31}$ as reported in the literature for branched PEI (Park and Choi, 1996), the viscosity average molecular mass ($\bar{M}_v$) for PEI used in this study was found to be 18 100 g/mol, which lies in between the $\bar{M}_w$ and $\bar{M}_n$ reported by the supplier.

The PEI adsorbed onto the nanoparticles was determined as $c_{ads} = c_i - c_f$, where c_{ads}, c_i, and c_f are the adsorbed, initial, and final concentrations in g/ml of PEI in the suspensions, respectively. The c_{ads} values were then used for calculating the PEI adsorbed per g of CNCs in the suspension, i.e., Γ_{ads} (mg/g). The plot of Γ_{ads} versus the C_{PEI}, amount of PEI (g/g CNC)

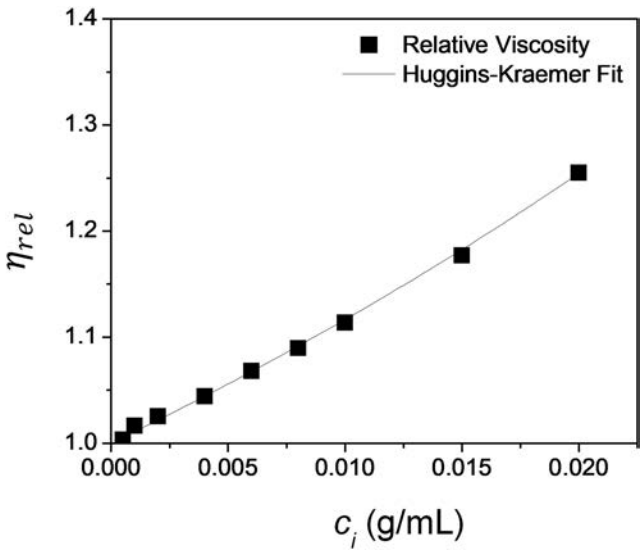

FIG. 1. Plot of relative viscosity η_{rel} as a function of the PEI concentration fitted to the Huggins-Kraemer equation.

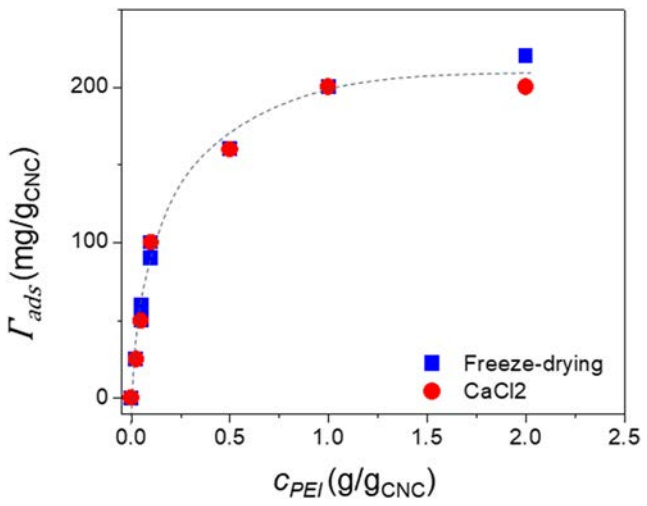

FIG. 2. The adsorption profile of PEI onto the CNC particles shown as a plot of PEI adsorbed [Γ_{ads} (mg/g$_{CNC}$)] versus the amount of PEI [c_{PEI} (g/g$_{CNC}$)] used in the preparation of aqueous CNC-PEI suspensions. PEI quantified in supernatant by (a) the calcium chloride method (circles) and (b) the freeze-drying method (squares).

used in the preparation of the suspensions, are presented in Fig. 2. Both the freeze-drying and calcium chloride methods of PEI determination in supernatant gave similar results with the maximum possible adsorption of PEI being around 200 mg per g of CNC. Similar to the adsorption of hydroxyethyl cellulose onto the CNCs (Lenfant *et al.*, 2017), the adsorption of PEI was also seen to follow the Langmuir model that can be expressed as

$$\Gamma_{ads} = \Gamma_{max} \frac{c_f}{c_f + k_a \Gamma_{max}}, \quad (2)$$

where Γ_{max} is the maximum adsorption possible and k_a is the absorption constant.

This study allowed the confirmation of the phenomenon of physical adsorption of PEI onto the CNCs. Thus, the adsorption of PEI onto the negatively charged CNCs is strong enough to withstand the electrostatic interactions from ionic species, i.e., Ca^{2+} and Cl^- ions (present up to 100 mM of salt concentration). While the maximum possible adsorption is about 200 mg of PEI per g of CNCs, the emphasis in the present study was on using low amounts of PEI in order to not significantly affect the morphology of the particle. This is an important criterion as a high degree of modification can affect the inherent attributes of the nanoparticles.

XPS and elemental analysis

The presence of PEI on the surface of the dried CNC-PEI particles was studied with XPS, a surface-sensitive technique. Table III shows the percent areas of C1s, N1s, and O1s peaks in the freeze-dried samples of unmodified CNC and CNC-PEI from CNC/PEI (1/0.02) and (3/0.02) suspensions. The CNC did not show any peaks for nitrogen and the percent areas of C1s and O1s resembled the signature peak profile of anhydroglucose, the monomer unit in cellulose. The percent ratio of oxygen to carbon in CNC-PEI samples was found to be lower than that in unmodified CNCs indicating the oxygen being masked by a PEI cover in the CNC-PEI particles. The N1s peak in CNC-PEI particles had a good signal to noise ratio in the high-resolution spectra and could be resolved into constituent peaks typical of unprotonated amine groups and to a very small degree of quaternized amine groups. Thus, the CNC-PEI particles do have some amine groups still protonated, which would explain the role of PEI in bridging interactions (refer to the sections titled DLS and zeta potential and Rheology characterization).

The X-rays in XPS penetrate to a sample depth of <10 nm, making it essentially a surface technique. If the coating of the PEI were to be ≥10 nm, the X-rays would only see the PEI layer and the N% and N/C percent ratio would resemble the theoretical N% and N/C ratio of PEI values (calculated from atomic mass of the elements in the molecular formula of PEI) as 32.6% and 0.58, respectively. However, we observe a N% and N/C ratio much lower implying that there is contribution from the carbon of cellulose and the X-rays can penetrate the

TABLE III. XPS data of percent area of C1s, O1s, and N1s peaks from high resolution spectra and the calculation of O/C, N%, and N/C ratio for the freeze-dried unmodified CNCs and CNC/PEI-0.02 samples. (i), (ii), and (iii) refer to the number of analyses: CNCs analyzed in duplicates and CNC/PEI-0.02 analyzed in triplicates.

Peak	CNC (i)	CNC (ii)	CNC/PEI-0.02 (i)	CNC/PEI-0.02 (ii)	CNC/PEI-0.02 (iii)
C1s C–O	40.3	41.3	38.7	42.2	41.9
O–C–O	6.3	6.2	7.6	6.4	6.4
N1s	No peak	No peak	0.6	0.6	0.6
O1s O–C	26.6	27.7	29.3	27	26.1
O–C–O	23.0	23.5	19.5	20.5	21.2
			Calculation		
O/C % ratio	1.07	1.08	1.06	0.98	0.98
N %	Zero	Zero	0.63	0.62	0.62
N/C % ratio	Zero	Zero	0.013	0.012	0.012

TABLE IV. The percentage of carbon, hydrogen, and nitrogen as analyzed from their respective peaks and the calculated N/C ratio for freeze-dried unmodified CNC and CNC/PEI-0.01(fd) and CNC/PEI-0.02(fd). (i) and (ii) refer to the number of analyses (samples analyzed in duplicates).

Sample	% C	% H	% N	N/C % ratio
CNC (i)	40.15	6.60	Absent	Zero
CNC (ii)	37.75	6.24	Absent	Zero
CNC/PEI-0.01 (i)	38.46	6.39	0.185	0.007
CNC/PEI-0.01 (ii)	40.99	6.76	0.199	0.007
CNC/PEI-0.02 (i)	37.06	6.23	0.446	0.014
CNC/PEI-0.02 (ii)	36.71	6.06	0.408	0.014

PEI coating to see the cellulose units beneath. Since the theoretical N% and N/C ratio for CNC/PEI-0.02 (calculated from the atomic mass of elements and the molecular mass of cellulose with 0.02 degree of substitution of PEI) would be 0.63% and 0.014, respectively, and the observed values are closer to these theoretical values, it can be inferred that the PEI is finely coated onto the CNCs and hence unlikely to affect the shape and structure of the CNCs.

The elemental analysis of the atomic percent in the CNC and CNC-PEI samples has been summarized in Table IV. The elemental analysis technique is not confined to the surface, and thus, the calculated atomic percent would be representative of the bulk of the given sample. The expected theoretical N% and N/C ratio for the CNC/PEI-0.01 would be 0.32% and 0.007, respectively, while for CNC/PEI-0.02, 0.63% and 0.014, respectively. The calculated N/C ratio in Table IV is similar to the theoretical values implying a uniform presence of PEI throughout the sample, which is also coherent with the XPS analysis.

TEM analysis

The TEM analysis of unmodified CNCs and CNC-PEI showed that the dimensions and shape of the particles were not changed after the modification. As seen from the TEM images in Fig. 3, there is hardly any difference between the two different particles in terms of shape. This corroborates the inference that was drawn from XPS and elemental analyses that the coating of PEI was very thin and did not affect the particle morphology. The dimensions of most particles as observed from these images were found to lie between 130 and 170 nm in length and 5-10 nm in width.

Rheological behavior

The 1% (w/w) CNC suspensions with varying amounts of PEI were found to be Newtonian with no storage modulus (G')

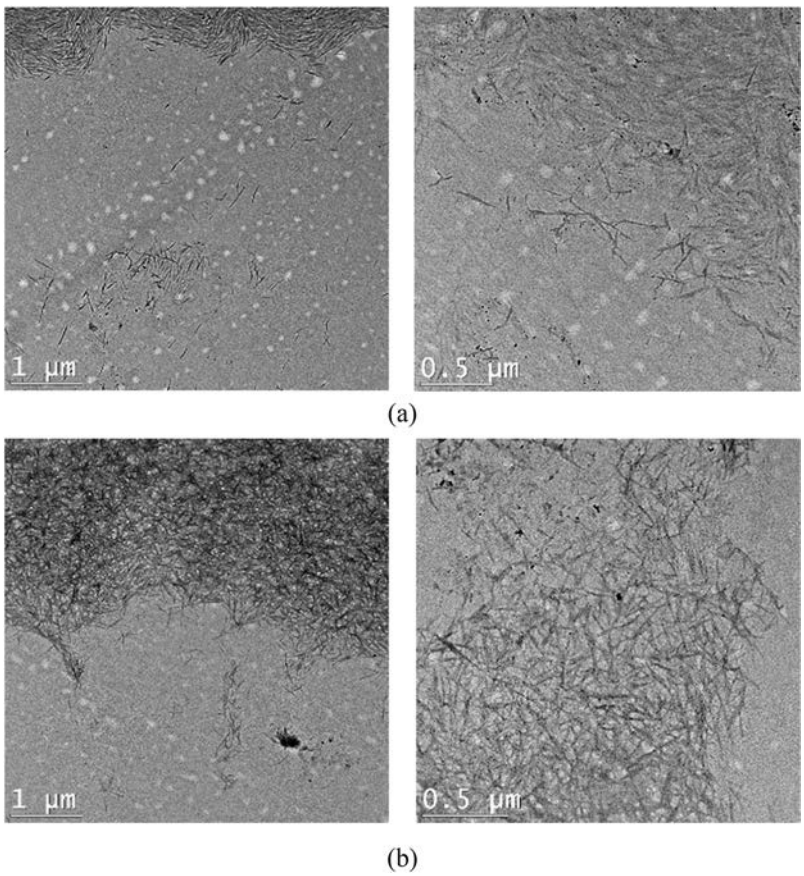

FIG. 3. TEM images at two magnifications of (a) unmodified CNCs and (b) CNC/PEI-0.02.

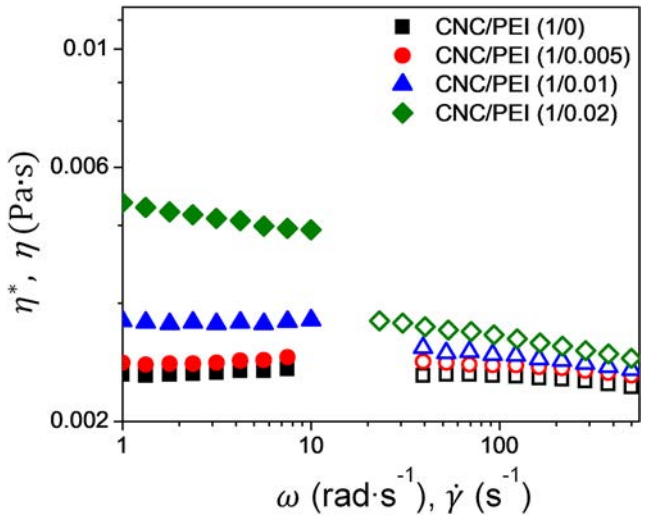

FIG. 4. Complex viscosity (filled symbols) and steady-shear viscosity (open symbols) as functions of the applied angular frequency (rad s^{-1}) and shear rate ($1\ s^{-1}$), respectively, for 1% (w/w) CNC suspensions made using different amounts of PEI (measurements done at 25 °C).

and a complex viscosity (η^*) independent of the applied angular frequency (ω). Figure 4 shows the complex viscosity and shear viscosity (η) plotted together for the applied angular frequency and shear rate ($\dot{\gamma}$) for 1% (w/w) CNC and CNC-PEI suspensions. The CNC/PEI (1/0.005) suspension showed negligible increases in the complex viscosity and marginal increases are noted for the CNC/PEI (1/0.01) sample. The CNC/PEI (1/0.02) suspension exhibits significant increases with a shear-thinning effect.

The incompliance to the Cox-Merz rule, i.e., $\eta^*(\omega) = \eta(\dot{\gamma})$ when $\omega \approx \dot{\gamma}$, for the steady state values can help ascertain inter-particle interaction in the suspension. The suspensions of unmodified CNCs and CNC/PEI (1/0.005) obey the Cox-Merz rule, implying the absence of any inter-particle interaction or network formation. The CNC/PEI (1/0.01) suspension shows the beginning of deviation from the Cox-Merz rule while CNC/PEI (1/0.02) clearly indicates the presence of bridging network associations that are lost under application of rotational shear deformation. The 1% (w/w) CNC suspensions are quite dilute and would have large inter-particle distance preventing any significant interactions or associations. However, in the CNC/PEI (1/0.02) suspension, the inter-particle distance would be reduced on account of an increase in particle size (as was observed in DLS study), thereby allowing for some degree of bridging effect.

The 3% (w/w) CNC suspension also behaves as a Newtonian fluid that did not show any evolution in the rheological parameters with time; however, the properties of the 3% (w/w) CNC-PEI suspensions were found to be time dependent. The freshly prepared 3% (w/w) CNC-PEI suspensions were Newtonian but turned into gel systems after a few hours. Thus, time sweep experiments were performed on the freshly prepared 3% (w/w) CNC-PEI suspensions to follow the gel formation. Figures 5(a) and 5(b) report the evolution of the storage modulus (G'), loss modulus (G''), and complex viscosity with time for the different CNC/PEI suspensions [note that there was no storage modulus for the Newtonian 3% (w/w) CNC suspension in Fig. 5(a)]. All suspensions containing PEI evolve the most in the first 10 h of being prepared and then reach a plateau where they continue to evolve, but at a much lower rate. They were found to never reach an equilibrium state where the rheology parameters became constant over time, and thus, the gel for each suspension was analyzed by frequency sweep. Several tests for any given composition were carried out and the values of the rheological parameters for any given composition were reproducible within ±20%.

Freshly prepared 3% (w/w) CNC-PEI suspensions have moduli and complex viscosity similar to the 3% (w/w) CNC suspension; however, with time, the storage modulus and complex viscosity of the CNC-PEI suspensions showed increase by almost three decades over 20 h, the storage

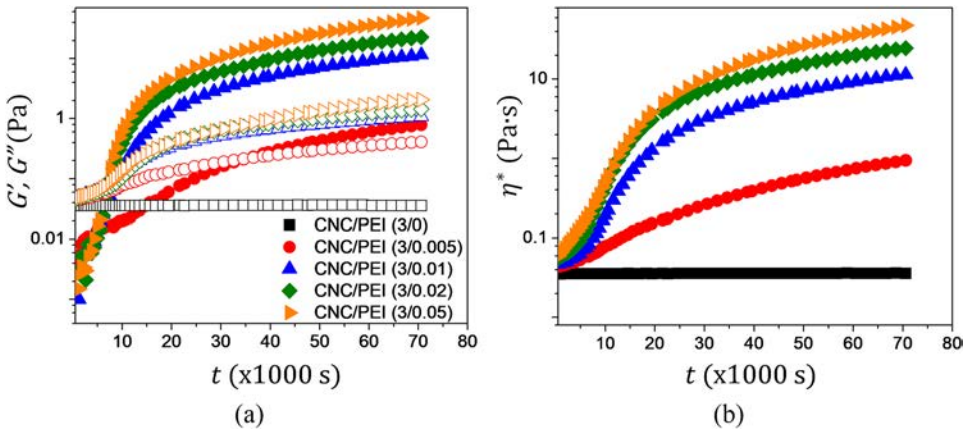

FIG. 5. Evolution of (a) storage modulus (filled symbols) and loss modulus (open symbols), and (b) complex viscosity during time sweep tests at 1 rad s^{-1} and 1% strain for the 3% (w/w) CNC suspensions having PEI 0.00, 0.005, 0.01, 0.02, and 0.05 g per g of CNCs(measurements done at 10 °C).

modulus being always greater than the loss modulus. The storage modulus values of CNC/PEI (3/0.01) are twice those of CNC/PEI (3/0.005), but the increase for CNC/PEI (3/0.02) and then CNC/PEI (3/0.05) was not to the same measure, implying a saturation point in the degree of inter-particle network for gel formation.

As expected, the gels formed are sensitive to the strain applied during time sweep experiments, as illustrated in Fig. 6 for the CNC/PEI (3/0.01). Figure 6(a) shows the time sweep done at 25% amplitude on CNC/PEI (3/0.01), and Figs. 6(b) and 6(c) show a comparison of the frequency sweep on the CNC/PEI (3/0.01) gel formed under time sweep at 1% and 25% amplitude. The system evolved into gel with similar time sweep profiles [Fig. 6(a)] having $G' > G''$ at 1 rad s^{-1} for both 1% and 25% amplitude; however, the resulting gel had different strength as seen from Fig. 6(b).

The strength of gels from the rheology perspective is understood in two ways: for weak gels, the storage modulus is dependent on applied frequency and the G' is <10 times of G'' (Clark and Ross-Murphy, 1987; Ikeda and Nishinari, 2001; and Picout and Ross-Murphy, 2003). As is apparent from frequency sweep in Fig. 6(b), the CNC/PEI (3/0.01) gel has a storage modulus always greater than the loss modulus over the entire frequency range, but when the system evolved into gel at strain of 25%, it had a lower G'/G'' ratio and larger variation in G' with increasing angular frequency than the gel formed at 1% amplitude. There is a significant difference in the loss modulus for the gel formed in 1% amplitude and 25% amplitude, implying a greater degree of network formation in the former. Since the networks or links between the CNC-PEI particles are not covalent in nature, they do rupture on higher frequency making the system flow. Thus, while the suspension evolved into a gel system in both cases with a similar sigmoidal evolution in time sweep, the rheological properties were different. The extent to which an inter-particle network could be achieved was apparently greater in soft conditions of 1% amplitude while a 25% strain was either preventing inter-particle associations or breaking some of them as they were formed, thereby resulting in a much weaker gel. For this reason, the suspensions were always allowed to evolve to the maximum extent and the time sweep was thereon performed at 1% strain. Figure 7 represents the rheological properties in the viscoelastic domain of the gel systems formed in Fig. 5 for different 3% (w/w) CNC-PEI suspensions.

From Fig. 7(a), it can be seen that the CNC/PEI (3/0.005) suspension does not really form a gel and there is a cross-over point between G' and G'' at around 10 rad s^{-1}. This suspension evolved into a thick but easily flowing paste. As the amount of PEI was increased to 0.01 g per g of CNC or more, there was a clear formation of gel with the G'/G'' [Fig. 7(b)] being maximum for CNC/PEI (3/0.05) at ~18 at 1 rad s^{-1}. Compared to the 3% (w/w) CNC suspension, the complex viscosity [Fig. 7(c)] of CNC-PEI (3/0.005) shows almost 2 decades of increase while the gel forming suspensions CNC-PEI (3/0.01) and (3/0.02) have four decades of increase.

The CNC/PEI gels were also studied in the non-linear viscoelastic domain by a shear "loop" involving application of increasing shear rate and decreasing shear rate. Figure 8 shows shear viscosity as a function of applied shear rate when the sequence of shear "loop" involves an increasing shear rate followed by a decreasing shear rate.

The CNC/PEI gels show a shear-thinning behavior on application of shearing which is not observed in the Newtonian 3% (w/w) CNC suspension. High concentrations of CNC suspensions [~5% (w/w) and above] are known to demonstrate a dependence of shear viscosity on applied $\dot{\gamma}$ where the viscosity decreases with increasing shear rate due to the orientation of the particles in the flow direction (Beuguel *et al.*, 2018b). The 3% (w/w) CNC suspension only suggestively shows this behavior (Fig. 8) as the low viscosity of

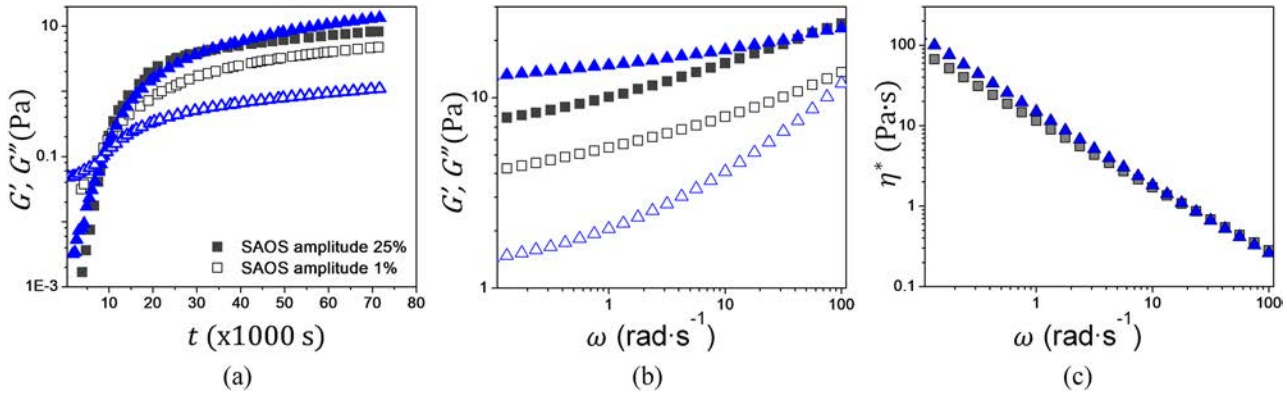

FIG. 6. (a) Time sweep data at 1 rad s^{-1} with 25% (gray symbols) and 1% (blue symbols) amplitude of CNC/PEI (3/0.01), (b) storage modulus (filled symbols) and loss modulus (open symbols), and (c) complex viscosity from the frequency sweep experiment in the linear viscoelastic domain for the CNC/PEI (3/0.01) gel formed during time sweep experiments (measurements done at 10 °C).

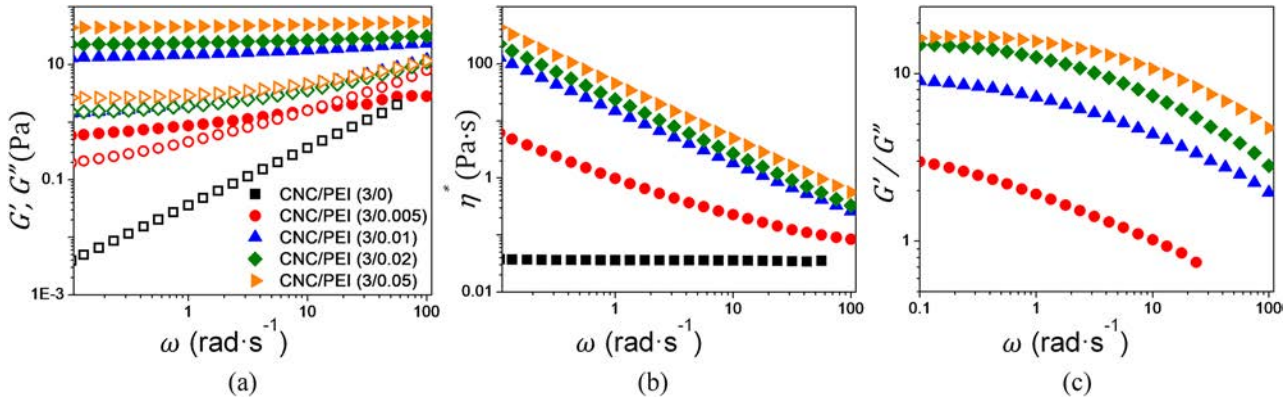

FIG. 7. The rheological parameters (a) storage modulus G' (filled symbols) and loss modulus G'' (open symbols), (b) G'/G'' ratio, and (c) complex viscosity (η^*) as a function of angular frequency (ω) in the linear viscoelastic domain for the gel systems of CNC/PEI (3/0), (3/0.005), (3/0.01), and (3/0.05) (measurements done at 10 °C).

the suspension allows for easy relaxation of the oriented CNCs.

The shear viscosity of the 3% (w/w) CNC suspension was found to be independent of the sequence in which increasing and decreasing shear rates were applied. However, as seen from Fig. 8, the CNC/PEI gels showed hysteresis in the viscosity values at low shear rates when the shear "loop" involved increasing shear rates followed by decreasing shear rates. Application of an increasing shear rate leads to a gradual breaking in network resulting in higher viscosity values than those from a decreasing shear rate where the inter-particle network does not reform fast-enough with reducing shear. When the shear "loop" involved a decreasing shear rate followed by an increasing shear rate, the shear viscosity values were similar for both, as the network was completely ruptured under high shearing at the initial stage of the experiment.

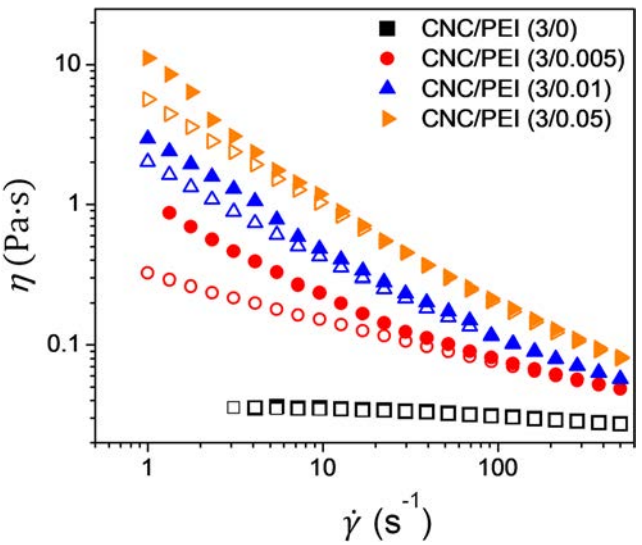

FIG. 8. Shear viscosity (η) versus shear rate ($\dot{\gamma}$) when a shear "loop" involved application of increasing shear rate (filled symbols) followed by a decreasing shear rate (open symbols) on CNC/PEI (3/0.00), (3/0.005), (3/0.01), and (3/0.05) (measurements done at 10 °C).

Also, the difference in shear viscosity values and the range of $\dot{\gamma}$ on the x-axis over which it is observed (Fig. 8) depends on the amount of PEI in the CNC/PEI gel. Trace amount of PEI in CNC/PEI (3/0.005) showed a larger difference over a longer range of $\dot{\gamma}$ (1–100 s^{-1}) while CNC/PEI (3/0.05) showed a smaller difference over a smaller range of $\dot{\gamma}$ (1–20 s^{-1}). To understand these observations in Fig. 8 of CNC/PEI gels, we need to consider the two dynamics involved during shearing, one concerning the slow relaxation of shear-oriented CNC particles due to high viscosity of the system and the other pertaining to the rupture of inter-particle bridging network. The viscosities of CNC/PEI (3/0.01), (3/0.02), and (3/0.05) gels are similar but much higher than 3% (w/w) CNC suspension; thus, the relaxation time of the oriented CNC particles would be similar for these gels and significantly greater than 3% (w/w) CNC suspension. The bridging network, however, would be to a greater extent in CNC/PEI (3/0.05) than in CNC/PEI (3/0.01), (3/0.02), or CNC/PEI (3/0.005) simply on account of the PEI content, the entity responsible for creating these inter-particle links. In the case of CNC/PEI (3/0.005), the system is a thick paste with a viscosity almost 2 decades more than 3% (w/w) CNC suspension and very little degree of inter-particle network due to trace amounts of PEI. Thus, the combination of the two phenomena, longer relaxation time of particles getting oriented in the direction of flow and the small degree of bridging network, results in a significant hysteresis between increasing shear rate and decreasing shear rate viscosities over a larger $\dot{\gamma}$ region of the graph (Fig. 8). On the other hand, the long relaxation time of particles oriented at high shear in CNC/PEI (3/0.05) is compensated by a greater degree of inter-particle network, which is reflected in a small

difference between the shear viscosities from the increasing shear rate and decreasing shear rate over a smaller $\dot{\gamma}$ region of the graph.

Figure 9 shows the plot of complex viscosity along with the shear viscosities from an increasing shear rate followed by a decreasing shear rate for different 3% (w/w) CNC-PEI compositions. The Cox-Merz rule is followed by the 3% (w/w) CNC suspensions but the viscoelastic gels of CNC/PEI show a deviation from this rule. The complex viscosity for these gels is always greater than the shear viscosity and the deviation is greater for higher PEI contents. Thus, PEI was responsible for the network formation that resulted in gels.

Figure 10 shows network re-formation in CNC/PEI (3/0.01) gel during 10 min and 30 min of rest after removal of shear. The CNC-PEI (3/0.01) gel was subjected to a shear "loop" of an increasing shear rate and a decreasing shear rate and then left undisturbed for 10 min. On application of an increasing shear rate again, the gel had an increase in shear viscosity due to re-establishment of some of the network during 10 min rest; however, it was still lower than what was initially obtained for the gel. When the system was allowed 30 min rest, the shear viscosity was similar to the initially obtained. To understand this re-gain in shear viscosity after 30 min of rest, an SAOS study was performed for different shear rates, which has been shown in Fig. 11.

It is obvious from the SAOS graph on the right side in Fig. 10 that the equilibrium structure before each SAOS depends on the magnitude of the pre-shear applied, wherein the greater is the pre-shear, the less developed is the structure (low G' values). After the removal of the shear, the structure re-establishes itself gradually and the G' increases with time. Since the lower pre-shear rate has a more developed structure, the SAOS is similar to the time sweep profile of the system in the plateau region. This behavior of the nanoparticles in polymer matrices had been previously demonstrated by Mobuchon *et al.* using organomodified clay in polybutene (Mobuchon *et al.*, 2007), and it was surprising to find this behavior for a suspension of surface functionalized CNCs at a dilute concentration of 3% (w/w).

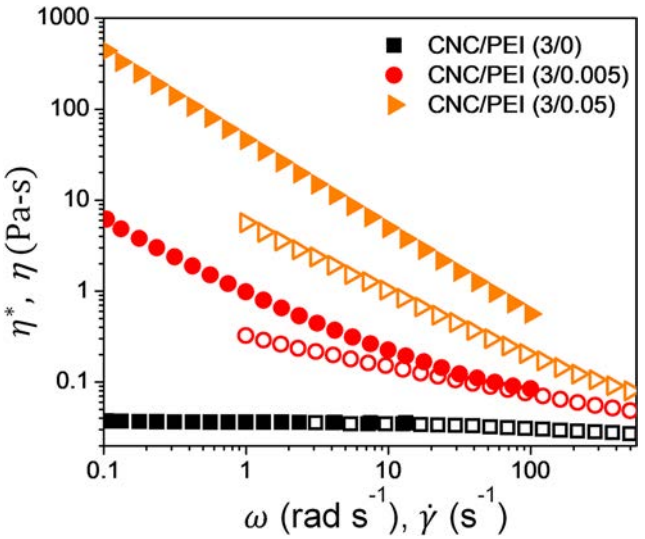

FIG. 9. Complex viscosity (η^*) (filled symbols) and the shear viscosity (η) (open symbols) from decreasing shear rate as a function of the applied angular frequency (ω) and shear rate ($\dot{\gamma}$), respectively, for CNC/PEI (3/0), (3/0.005), and (3/0.05) (measurements done at 10 °C).

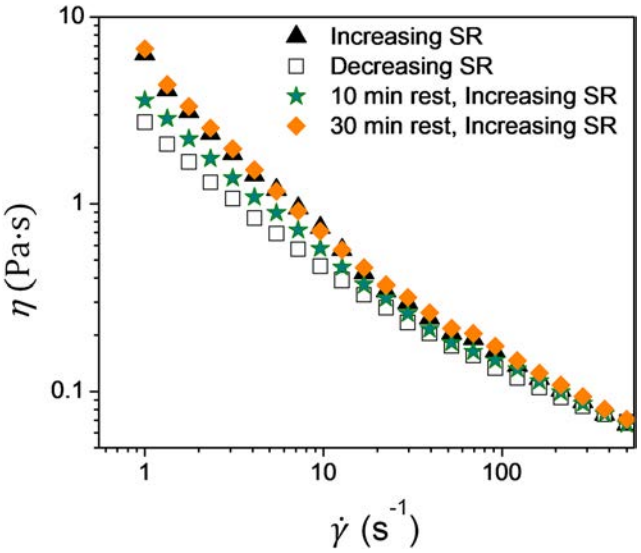

FIG. 10. Shear viscosity (η) versus the applied shear rate ($\dot{\gamma}$) for the gel of CNC/PEI (3/0.01) when shearing is applied: increasing shear rate, decreasing shear rate, rest of 10 min followed by increasing shear rate, and rest of 30 min followed by increasing shear rate (measurements done at 10 °C).

Re-dispersion of freeze-dried particles in water

This surface modification is based on physical adsorption of PEI, which has an affinity for negatively charged CNCs. However, since PEI is water soluble, it also has a strong affinity for water. Physical adsorption processes can be reversible in nature and thus, to understand if this modification is also reversible, the freeze-dried particles obtained from aqueous suspension were re-suspended in water. Figure 11(a) shows that freeze-dried CNCs can be re-suspended in water, but the CNC-PEI particles cannot re-suspended in water, implying the modification to be irreversible.

It is surprising that these CNC-PEI particles do not show any phase separation in their freshly prepared suspensions, but once dried cannot be re-suspended in water (Fig. 12). The reason for this is as yet unknown; however, we posit that, during preparation of the CNC/PEI suspensions, when the PEI solution is introduced to the well suspended CNCs in water,

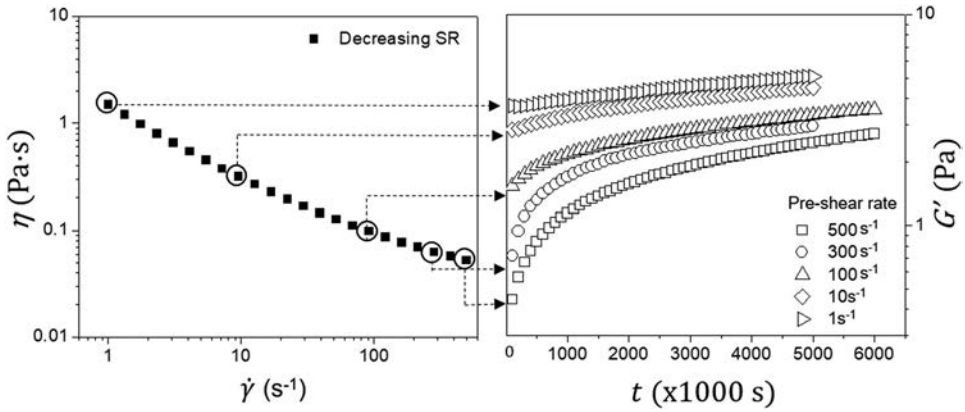

FIG. 11. Structure evolution in CNC/PEI (3/0.01) gel: (a) shear viscosity (η) versus decreasing shear rate ($\dot{\gamma}$) followed by (b) an SAOS at 1 rad s^{-1} and 1% amplitude at steady state for different pre-shear (measurements done at 10 °C).

the modification in aqueous suspensions would likely have the PEI chains well extended in water along with some water molecules possibly trapped between the physically adsorbed PEI and CNCs. This would allow the suspension to remain stable on account of proper interaction with the solvent, despite having a reduced surface charge. However, once freeze-dried, the water molecules are removed and the PEI chains would likely collapse onto the CNC surface resulting in much greater contact between the two entities. Given that the electrostatic force is a strong interaction, the re-introduction of water is unlikely to reduce the CNC-PEI interactions and, hence, now the water molecules can be imagined to be interacting with only PEI on the CNC surface that would appear less hydrophilic from charge neutralized ethyleneimine groups.

The CNC-PEI particles studied in the present work are made using low amounts of PEI that never result in complete charge neutralization of the CNC surface (recall the zeta potential analysis). Thus, these particles only have reduced hydrophilicity from lower surface charge rather than have a hydrophobic surface due to completely charge neutralized PEI on the CNC. As a result, no noticeable difference in the dispersion of freeze-dried CNC and CNC-PEI particles was observed in non-polar solvents (e.g., toluene, hexane).

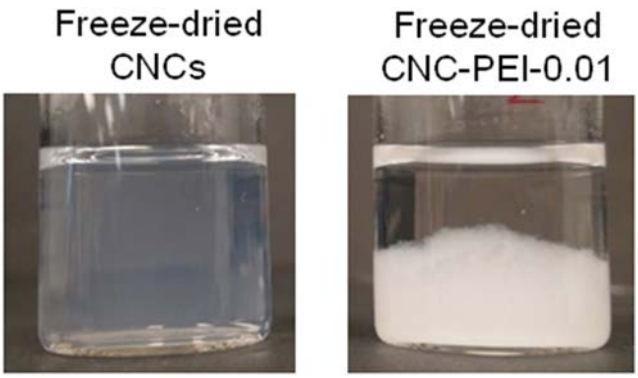

FIG. 12. Behavior of freeze-dried CNCs and freeze-dried CNC-PEI-0.01 in water after ultrasonication treatment.

CONCLUDING REMARKS

The present study is relevant for two aspects, one being the uniform non-covalent surface modification of CNCs in an aqueous medium without the use of any catalyst and coupling agent and the second being the formation of gel by the suspensions of the modified CNCs. The modification of the negatively charged CNCs relies on physical adsorption of cationic branched polymer PEI on account of electrostatic attraction. The use of ultrasonication during the modification allows for a uniform coating of the particles and the resulting aqueous suspensions are stable without phase separation for days. The XPS and elemental analyses confirmed the uniformity of PEI coating, while the TEM images showed that the shape of nanoparticles was not affected as a result of this coating.

The Newtonian 3% (w/w) CNC suspension evolved into a non-Newtonian gel system when the CNCs were modified with an amount of PEI that is only one hundredth of the total CNCs in the suspension. The non-covalent inter-particle interactions due to bridging networks formed by PEI could be broken down by the application of shear, but were re-established on removal of shear to result in the same rheological parameters as of the original gel, but after very long times.

This study demonstrates how to make non-covalent modification efficient in terms of uniformly modifying CNCs without agglomerates while opening up avenues of fine-tuning CNC suspension properties for various end-use applications such as hydrogels with self-healing properties, pharmaceutical formulations, and viscosity modifiers.

ACKNOWLEDGMENTS

CelluForce is acknowledged for providing the CNCs. We also thank NSERC, PRIMA Québec, and FPInnovations for their financial support. The authors are grateful to Dr. Wadood Hamad of FPInnovations for his helpful suggestions.

REFERENCES

Abitbol, T., Johnstone, T., Quinn, T. M., and Gray, D. G., "Reinforcement with cellulose nanocrystals of poly(vinyl alcohol) hydrogels prepared by cyclic freezing and thawing," Soft Matter **7**, 2373–2379 (2011).

Alexandrescu, L., Syverud, K., Gatti, A., and Chinga-Carrasco, G., "Cytotoxicity tests of cellulose nanofibril-based structures," Cellulose **20**, 1765–1775 (2013).

Azevedo, M. M., Ramalho, P., Silva, A. P., Teixeira-Santos, R., Pina-Vaz, C., and Rodrigues, A. G., "Polyethyleneimine and polyethyleneimine-based nanoparticles: Novel bacterial and yeast biofilm inhibitors," J. Med. Microbiol. **63**, 1167–1173 (2014).

Bagheriasl, D., Carreau, P. J., Riedl, B., Dubois, C., and Hamad, W., "Shear rheology of polylactide (PLA)–cellulose nanocrystal (CNC) nanocomposites," Cellulose **23**, 1885–1897 (2016).

Beck, S., Bouchard, J., and Berry, R., "Dispersibility in water of dried nanocrystalline cellulose," Biomacromolecules **13**, 1486–1494 (2012).

Beuguel, Q., Tavares, J. R., Carreau, P. J., and Heuzey, M.-C., "Rheological behavior of cellulose nanocrystal suspensions in polyethylene glycol," J. Rheol. **62**, 607–618 (2018a).

Beuguel, Q., Tavares, J. R., Carreau, P. J., and Heuzey, M.-C., "Ultrasonication of spray- and freeze-dried cellulose nanocrystals in water," J. Colloid Interface Sci. **516**, 23–33 (2018b).

Cao, Y., Zavattieri, P., Youngblood, J., Moon, R., and Weiss, J., "The relationship between cellulose nanocrystal dispersion and strength," Constr. Build. Mater. **119**, 71–79 (2016).

Clark, A. H. and Ross-Murphy, S. B., "Structural and mechanical properties of biopolymer gels," Adv. Polym. Sci. **83**, 57–192 (1987).

Dong, S. P. and Roman, J. M., "Fluorescently labeled cellulose nanocrystals for bioimaging applications," Am. Chem. Soc. **129**, 13810–13811 (2007).

Ehmann, H. M. A., Mohan, T., Koshanskaya, M., Scheicher, S., Breitwieser, D., Ribitsch, V., Stana-Kleinschekd, K., and Spirk, S., "Design of anticoagulant surfaces based on cellulose nanocrystals," RSC Chem. Commun. **50**, 13070–13072 (2014).

Eyley, S. and Thielemans, W., "Surface modification of cellulose nanocrystals," Nanoscale **6**, 7764–7779 (2014).

France, K. J. D., Hoare, T., and Cranston, E. D., "Review of hydrogels and aerogels containing nanocellulose," Chem. Mater. **29**, 4609–4631 (2017).

Girouard, N., Schueneman, G. T., Shofner, M. L., and Meredith, J. C., "Exploiting colloidal interfaces to increase dispersion, performance, and pot-life in cellulose nanocrystal/waterborne epoxy composites," Polymer **68**, 111–121 (2015).

Girouard, N., Xu, S., Schueneman, G. T., Shofner, M. L., and Meredith, J. C., "Site-selective modification of cellulose nanocrystals with isophorone diisocyanate and formation of polyurethane-CNC composites," ACS Appl. Mater. Interfaces **8**, 1458–1467 (2016).

Guise, C. and Fangueiro, R., "Biomedical applications of nanocellulose," in *Natural Fibres: Advances in Science and Technology towards Industrial Applications*, Volume 12 of RILEM Bookseries, edited by Fangueiro, R. and Rana, S. (Springer, Dordrecht, 2016).

Habibi, Y., Lucia, L. A., and Rojas, O. J., "Cellulose nanocrystals: Chemistry, self-assembly, and applications," ACS Chem. Rev. **110**, 3479–3500 (2010).

Hasani, M., Cranston, E. D., Westman, G., and Gray, D. G., "Cationic surface functionalization of cellulose nanocrystals," Soft Matter **4**, 2238–2244 (2008).

Heux, L., Bonini, C., Cavaille, J. Y., Linder, P., Dewhurst, C., and Terech, P., "Rodlike cellulose whiskers coated with surfactant: A small-angle neutron scattering characterization," Langmuir **18**, 3311–3314 (2002).

Hoeger, I., Rojas, O. J., Efimenko, K., Velev, O. D., and Kelley, S. S., "Ultrathin film coatings of aligned cellulose nanocrystals from a convective-shear assembly system and their surface mechanical properties," Soft Matter **7**, 1957–1967 (2011).

Hu, Z., Ballinger, S., Pelton, R., and Cranston, E. D., "Surfactant-enhanced cellulose nanocrystal Pickering emulsions," J. Colloid Interface Sci. **439**, 139–148 (2015).

Ikeda, S. and Nishinari, K., "'Weak gel'-type rheological properties of aqueous dispersions of nonaggregated K-carrageenan helices," J. Agric. Food Chem. **49**, 4436–4441 (2001).

Javanbakht, T., Raphael, W., and Tavares, J. R., "Physicochemical properties of cellulose nanocrystals treated by photo-initiated chemical vapour deposition (PICVD)," Can. J. Chem. Eng. **94**, 1135–1139 (2016).

Jia, H., Pu, W.-F., Zhao, J.-Z., and Jin, F.-Y., "Research on the gelation performance of low toxic PEI cross-linking PHPAM gel systems as water shutoff agents in low temperature reservoirs," Ind. Eng. Chem. Res. **49**, 9618–9624 (2010).

Jorfi, M., Roberts, M. N., Foster, E. J., and Weder, C., "Physiologically responsive, mechanically adaptive bio-nanocomposites for biomedical applications," ACS Appl. Mater. Interfaces **5**, 1517–1526 (2013).

Kaboorani, A. and Riedl, B., "Surface modification of cellulose nanocrystals (CNC) by a cationic surfactant," Ind. Crops Prod. **65**, 45–55 (2015).

Kalashnikova, I., Bizot, H., Bertoncini, P., Cathala, B., and Capron, I., "Cellulosic nanorods of various aspect ratios for oil in water Pickering emulsions," Soft Matter **9**, 952–959 (2013).

Kalia, S., Dufresne, A., Cherian, B. N., Kaith, B. S., Avérous, L., Njuguna, J., and Nassiopoulos, E., "Cellulose-based bio- and nanocomposites: A review," Int. J. Polym. Sci. **2011**, 1–35.

Kobayashi, S., Hiroishi, K., Tokunoh, M., and Saegusa, T., "Chelating properties of linear and branched poly(ethy1enimines)," Macromolecules **20**, 1496–1500 (1987).

Lenfant, G., Heuzey, M.-C., van de Ven, T. G. M., and Carreau, P. J., "Gelation of crystalline nanocellulose in the presence of hydroxyethyl cellulose," Can. J. Chem. Eng. **95**, 1891–1900 (2017).

Lewis, L., Derakhshandeh, M., Hatzikiriakos, S. G., Hamad, W. Y., and MacLachlan, M. J., "Hydrothermal gelation of aqueous cellulose nanocrystal suspensions," Biomacromolecules **17**(8), 2747–2754 (2016).

Li, M.-C., Mei, C., Xu, X., Lee, S., and Wu, Q., "Cationic surface modification of cellulose nanocrystals: Toward tailoring dispersion and interface in carboxymethyl cellulose films," Polymer **107**, 200–210 (2016).

Lin, N. and Dufresne, A., "Nanocellulose in biomedicine: Current status and future prospect," Eur. Polym. J. **59**, 302–325 (2014).

Marchessault, R. H., Morehead, F. F., and Walter, N. M., "Liquid crystal systems from fibrillar polysaccharides," Nature **184**, 632–633 (1959).

Meulendijks, N., Burghoorn, M., Ee, R. V., Mourad, M., Mann, D., Keul, H., Bex, G., Veldhoven, E. V., Verheijen, M., and Buskens, P., "Electrically conductive coatings consisting of Ag-decorated cellulose nanocrystals," Cellulose **24**, 2191–2204 (2017).

Millon, L. E. and Wan, W. K., "The polyvinyl alcohol–bacterial cellulose system as a new nanocomposite for biomedical applications," J. Biomed. Mater. Res., Part B **79B**, 245–253 (2006).

Mobuchon, C., Carreau, P. J., and Heuzey, M.-C., "Effect of flow history on the structure of a non-polar polymer/clay nanocomposite model system," Rheol. Acta **46**, 1045–1056 (2007).

Moon, R. J., Martini, A., Nairn, J., Simonsen, J., and Youngblood, J., "Cellulose nanomaterials review: Structure, properties and nanocomposites," Chem. Soc. Rev. **40**, 3941–3994 (2011).

Ortega-MuCoz, M., Giron-Gonzalez, M. D., Salto-Gonzalez, R., Jodar-Reyes, A. B., De Jesus, S. E., Lopez-Jaramillo, F. J., Hernandez-Mateo, F., and Santoyo-Gonzalez, F., "Polyethyleneimine-coated gold nanoparticles: Straightforward preparation of efficient DNA delivery nanocarriers," Chem. - Asian J. **11**, 3365–3375 (2016).

Park, H. I. and Choi, E.-J., "Characterization of branched polyethyleneimine by laser light scattering and viscometry," Polymer **37**, 313–319 (1996).

Peresin, M. S., Vesterinen, A.-H., Habibi, Y., Johansson, L.-S., Pawlak, J. J., Nevzorov, A. A., and Rojas, O. J., "Crosslinked PVA nanofibers reinforced with cellulose nanocrystals: Water interactions and thermomechanical properties," J. Appl. Polym. Sci. **131**, 40334 (2014).

Picout, D. R. and Ross-Murphy, S. B., "Rheology of biopolymer solutions and gels," Sci. World J. **3**, 105–121 (2003).

Podgornik, R., "Polyelectrolyte-mediated bridging interactions," J. Polym. Sci., Part B: Polym. Phys. **42**, 3539–3556 (2004).

Poptoshev, E. and Claesson, P. M., "Forces between glass surfaces in aqueous polyethylenimine solutions," Langmuir **18**, 2590–2594 (2002).

Reddy, B. R., Eoff, L., Dalrymple, E. D., Black, K., Brown, D., and Rietjens, M., "A natural polymer-based cross-linker system for conformance gel systems," Soc. Pet. Eng. **8**, 99–103 (2003).

Sabra, A., Anderson, P. J., Carson, M., Shuja, A., Sunasee, R., and Ckless, K., "Immunological and oxidative responses caused by cellulose nanocrystal (CNCs) derivatives designed for biomedical applications, in human and mouse cells," Free Radical Biol. Med. **112**, 209–210 (2017).

Sojoudiasli, H., Heuzey, M.-C., and Carreau, P. J., "Mechanical and morphological properties of cellulose nanocrystal-polypropylene composites," Polym. Compos. **16**, 101–113 (2017).

Smits, R. G., Koper, G. J. M., and Mandel, M., "The influence of nearest- and next-nearest-neighbor interactions on the potentiometric titration of linear poly(ethyleneimine)," J. Phys. Chem. **97**, 5745–5751 (1993).

Suh, J., Paik, H.-J., and Hwang, B. K., "Ionizationof poly(ethyleneimine) and poly(allylamine) at various pH's," Bioorg. Chem. **22**, 318–327 (1994).

Sun, S. P., Hatton, P. A., and Chung, T.-S., "Hyperbranched polyethyleneimine induced cross-linking of polyamide-imide nanofiltration hollow fiber membranes for effective removal of ciprofloxacin," Environ. Sci. Technol. **45**, 4003–4009 (2011).

Vancha, A. R., Govindaraju, S., Parsa, K. V. L., Jasti, M., González-García, M., and Ballestero, R. P., "Use of polyethyleneimine polymer in cell culture as attachment factor and lipofection enhancer," BMC Biotechnol. **4**, 23 (2004).

Wang, C. J., Chen, C., Ren, H., Yang, Y., and Dai, H., "Polyethyleneimine addition for control of dissolved and colloidal substances: Effects on wet-end chemistry," BioResources **11**, 9756–9770 (2016).

Wena, C., Yuana, Q., Lianga, H., and Vriesekoop, F., "Preparation and stabilization of d-limonene pickering emulsions by cellulose nanocrystals," Carbohydr. Polym. **112**, 695–700 (2014).

Xia, T., Kovochich, M., Liong, M., Meng, H., Kabehie, S., Zink, J. I., and Nel, A. E., "Polyethyleneimine coating enhances the cellular uptake of mesoporous silica nanoparticles and allows safe delivery of siRNA and DNA constructs," ACS Nano **3**, 3273–3286 (2009).

Xu, Q. X., Yi, J., Zhang, X. F., and Zhang, H. L., "A novel amphotropic polymer based on cellulose nanocrystals grafted with azo polymers," Eur. Polym. J. **44**, 2830–2837 (2008).

Yang, D., Peng, X., Zhong, L., Cao, X., Chen, W., Wang, S., Liu, C., and Sun, R., "Fabrication of highly elastic nanocomposite hydrogel by surface modification of cellulose nanocrystal," RSC Adv. **5**, 13878–13885 (2015).

Zhao, J., Li, Q., Zhang, X., Xiao, M., Zhang, W., and Lu, C., "Grafting of polyethylenimine onto cellulose nanofibers for interfacial enhancement in their epoxy nanocomposites," Carbohydr. Polym. **157**, 1419–1425 (2017).